
Amyloid Imaging with ^{18}F -Florbetaben in Alzheimer Disease and Other Dementias

Victor L. Villemagne¹⁻³, Kevin Ong^{1,2}, Rachel S. Mulligan¹, Gerhard Holl⁴, Svetlana Pejoska¹, Gareth Jones¹, Graeme O'Keefe¹, Uwe Ackerman¹, Henri Tochon-Danguy¹, J. Gordon Chan¹, Cornelia B. Reininger⁴, Lueder Fels⁴, Barbara Putz⁴, Beate Rohde⁴, Colin L. Masters³, and Christopher C. Rowe^{1,2}

¹Department of Nuclear Medicine and Centre for PET, Austin Health, Heidelberg, Victoria, Australia; ²Department of Medicine, University of Melbourne, Parkville, Victoria, Australia; ³The Mental Health Research Institute of Victoria, Parkville, Victoria, Australia; and ⁴Bayer Schering Pharma, Berlin, Germany

Amyloid imaging with ^{18}F -labeled radiotracers will allow widespread use, facilitating research, diagnosis, and therapeutic development for Alzheimer disease. The purpose of the study program was to compare cortical amyloid deposition using ^{18}F -florbetaben and PET in controls and subjects with mild cognitive impairment (MCI), frontotemporal lobar degeneration (FTLD), dementia with Lewy bodies (DLB), vascular dementia (VaD), Parkinson disease (PD), and Alzheimer disease (AD).

Methods: One hundred nine subjects in 3 clinical studies at Austin Health were reviewed: 32 controls, 20 subjects with MCI, and 30 patients with AD, 11 with FTLD, 7 with DLB, 5 with PD, and 4 with VaD underwent PET after intravenous injection of 300 MBq of ^{18}F -florbetaben. Standardized uptake value ratios (SUVR) using the cerebellar cortex as a reference region were calculated between 90 and 110 min after injection. **Results:** When compared with the other groups, AD patients demonstrated significantly higher SUVRs ($P < 0.0001$) in neocortical areas. Most AD patients (96%) and 60% of MCI subjects showed diffuse cortical ^{18}F -florbetaben retention. In contrast, only 9% of FTLD, 25% of VaD, 29% of DLB, and no PD patients and 16% of controls showed cortical binding. Although there was a correlation between Mini Mental State Examination and β -amyloid burden in the MCI group, no correlation was observed in controls, FTLD or AD. **Conclusion:** ^{18}F -florbetaben had high sensitivity for AD, clearly distinguished patients with FTLD from AD, and provided results comparable to those reported with ^{11}C -Pittsburgh Compound B in a variety of neurodegenerative diseases.

Key Words: Alzheimer disease; amyloid imaging; $\text{A}\beta$; positron emission tomography; frontotemporal dementia; dementia with Lewy bodies; neurodegenerative disorders

J Nucl Med 2011; 52:1210–1217

DOI: 10.2967/jnumed.111.089730

β -amyloid ($\text{A}\beta$) imaging with PET permits in vivo assessment of $\text{A}\beta$ deposition in the brain, providing an important new tool for the evaluation of the causes, diagnosis,

and future treatment of dementias for which $\text{A}\beta$ may play a role (1). Studies with ^{11}C -Pittsburgh Compound B (^{11}C -PiB), the most specific and most widely used PET $\text{A}\beta$ ligand, indicate that $\text{A}\beta$ imaging may allow earlier diagnosis of Alzheimer disease (AD) pathology (2–4) and accurate differential diagnosis of the dementias (2,5,6). ^{11}C -PiB studies show robust cortical binding in almost all AD patients (2,3) and correlate well with reduction in cerebrospinal fluid $\text{A}\beta_{42}$ (7). Binding is associated with cerebral atrophy as measured by MRI (8) and with episodic memory impairment in apparently healthy elderly individuals and in subjects with mild cognitive impairment (MCI) (9). Increased ^{11}C -PiB binding may also be predictive of conversion of MCI to AD (10).

After recent advances in imaging and cerebrospinal fluid analysis, it has been proposed that the research criteria for the diagnosis of probable AD should be revised to allow earlier diagnosis and therapeutic intervention. These proposals have argued that when there is a clear history of progressive cognitive decline, objective evidence from psychometric tests of episodic memory impairment, and characteristic abnormalities in the cerebrospinal fluid or neuroimaging studies such as amyloid imaging, dementia might not be required for the diagnosis of probable AD (11,12). Thus, as the criteria for the diagnosis of AD evolve, $\text{A}\beta$ imaging is likely to have an increasingly important role in clinical practice provided it is accessible and affordable (13).

Unfortunately, the 20-min radioactive decay half-life of ^{11}C limits the use of ^{11}C -PiB to centers with an on-site cyclotron and ^{11}C radiochemistry expertise. Consequently, access to ^{11}C -PiB PET is restricted, and the high cost of studies is prohibitive for routine clinical use. To overcome these limitations, several tracers labeled with ^{18}F (half-life, 110 min), permitting centralized production and regional distribution, were synthesized and tested (13–17).

We reported in the first human study with ^{18}F -florbetaben (^{18}F -BAY94-9172) (14) a robust separation in 15 AD patients from 15 healthy age-matched controls and 5 frontotemporal lobar degeneration (FTLD) patients both by visual image

Received Feb. 23, 2011; revision accepted May 9, 2011.

For correspondence or reprints contact: Victor L. Villemagne, Department of Nuclear Medicine and Centre for PET, Austin Health, 145 Studley Rd., Heidelberg, Victoria, 3084, Australia.

E-mail: villemagne@petnm.unimelb.edu.au

COPYRIGHT © 2011 by the Society of Nuclear Medicine, Inc.

interpretation and simple quantitative measures from a scan that requires 20 min of PET camera time. The continuation of this study and the additional studies aim at extending those initial evaluations into other dementing and nondementing neurodegenerative diseases and compare the results with clinical and cognitive features.

MATERIALS AND METHODS

Study Participants

The studies were approved by the Austin Health Human Research Ethics Committee. Written informed consent was obtained from all subjects before participation and also from the next of kin or caregiver for the patients with dementia. Participants were clinically classified by consensus between a neurologist and a neuropsychologist. Thirty-two controls; 20 patients meeting criteria for MCI, with 80% of them being classified as amnesic MCI (18); 30 patients meeting the National Institute of Neurological Disorders and Stroke–Alzheimer’s Disease and Related Disorders Association criteria for probable AD (19); 11 patients with consensus criteria for FTLD (20); 7 patients meeting criteria for dementia with Lewy bodies (DLB) (21); 5 patients with Parkinson disease (PD) (22); and 4 patients meeting National Institute of Neurological Disorders and Stroke–Association Internationale pour la Recherche et l’Enseignement en Neurosciences criteria for vascular dementia (VaD) (23) were studied. Subjects with probable dementia or MCI were recruited from the Austin Health Memory Disorders Clinic if they met the inclusion and exclusion criteria and were willing to participate. Participants fulfilling clinical criteria for PD were recruited from movement disorders clinics. Controls were recruited by advertisement in the community. Data from half of the controls, half of the AD, and FTLD patients included into the first human study have appeared in a previous report (14).

All subjects were aged over 55 y, spoke fluent English, and had completed at least 7 y of education. No subjects had a history or physical or imaging findings of other neurologic or psychiatric illness, current or recent drug or alcohol abuse or dependence, or any significant other disease or unstable medical condition.

Participants were administered the Mini Mental State Examination (MMSE), the Clinical Dementia Rating (CDR), and a battery of neuropsychologic tests to ensure patients fulfilled diagnostic criteria for AD or normality. Controls were excluded if any score fell below 1 SD of the published mean for that test. MRI and psychometric examination were completed within 4 wk of the ^{18}F -florbetaben scan.

As previously reported (14), safety monitoring consisted of hematology and biochemistry assessments, clinical observation, and intermittent measurement of vital signs for 3 h commencing immediately before tracer injection. Clinical and laboratory evaluation was repeated 1 wk after the scan for comparison. Participants were asked about possible adverse events at 24 h and 1 wk after injection.

Image Acquisition

MRI consisted of a 3-dimensional T1-weighted magnetization-prepared rapid gradient-echo scan (repetition time, 2,300 ms; echo time, 2.98 ms; and flip angle, 9°) used for screening and coregistration with the PET images. The image size was $160 \times 240 \times 256$ voxels, with a voxel dimension of $1.2 \times 1 \times 1$ mm in the sagittal, coronal, and axial directions, respectively. All high-resolution MR images were obtained on a 3-T Magnetom Trio scanner (Siemens).

^{18}F -florbetaben was radiolabeled in the Centre for PET, Austin Health, as previously described (14). The final administered product contained 1.6 ± 1.2 μg of florbetaben, with a specific activity (SA) of 105 ± 74 GBq/ μmol and a radiochemical purity higher than 95%. PET scans were acquired on a 3-dimensional Phillips Allegro scanner in the Austin Health Centre for PET. A transmission scan using a rotating ^{137}Cs source was obtained for attenuation correction immediately before the emission scan. Although some subjects underwent a dynamic acquisition scan for 60 min after injection of 300 MBq of ^{18}F -florbetaben, all participants underwent a static scan at 90–110 min after injection. Images were reconstructed using a 3-dimensional row-action maximum-likelihood algorithm.

To test the robustness of the results and potential pharmacologic effects of florbetaben, a subgroup of 8 controls and 8 AD patients underwent a second PET scan within 4 wk (median, 3 wk), for which 50 μg of florbetaben were added to the end-of-synthesis solution. Thus, the administered final product contained 1.9 ± 0.9 μg of florbetaben with an SA of 58.4 ± 27.5 GBq/ μmol for the high-SA study and 49.4 ± 3.1 μg of florbetaben with an SA of 1.9 ± 0.2 GBq/ μmol for the low-SA study; in both studies, radiochemical purity was higher than 95%.

Image Analysis

PET images were coregistered with each individual’s MR image using SPM5 (24). Regions of interest (ROIs) were then drawn on the individual MR image and transferred to the coregistered PET images (Fig. 1). Mean radioactivity values were obtained from ROIs for cortical, subcortical, and cerebellar regions. White-matter ROIs were placed at the centrum semiovale, and the cerebellar regions were placed over the cerebellar cortex, with care taken to avoid white matter (Fig. 1). In 4 patients, MR images could not be obtained and ROIs were drawn directly onto the PET images by an operator unaware of the clinical status of the patients. No correction for partial volume was applied to the PET data.

Standardized uptake values (SUVs), defined as the decay-corrected brain radioactivity concentration, normalized for injected dose and body weight, were calculated for all regions. These were then used to derive the SUV ratio (SUVR) referenced to the cerebellar cortex, a region relatively unaffected by dense A β plaques in sporadic AD, at 90 min after injection, when the ratio of binding in the neocortex to that in the cerebellar cortex reaches apparent steady-state (14). Neocortical A β burden was expressed as the average SUVR of the area-weighted mean for the following cortical ROIs: frontal (consisting of dorsolateral prefrontal, ventrolateral prefrontal, and orbitofrontal regions), superior parietal, lateral temporal, lateral occipital, and anterior and posterior cingulate.

To identify an SUVR cutoff, a hierarchical cluster analysis was performed on the controls that yielded a cutoff for high or low neocortical SUVR of 1.4, similar to the cutoff values used in previous PiB PET studies (8,25).

The ^{18}F -florbetaben 90- to 110-min SUVR images were also visually graded on a Philips workstation and displayed with a rainbow color scale. The color scale was adjusted so that cerebellar white matter was yellow, as previously described for reading ^{11}C -PiB images (26). Two nuclear medicine physicians with experience in interpretation of ^{11}C -PiB scans and unaware of diagnosis and all other clinical information classified the ^{18}F -florbetaben images as normal, possible A β deposition, or probable A β deposition based

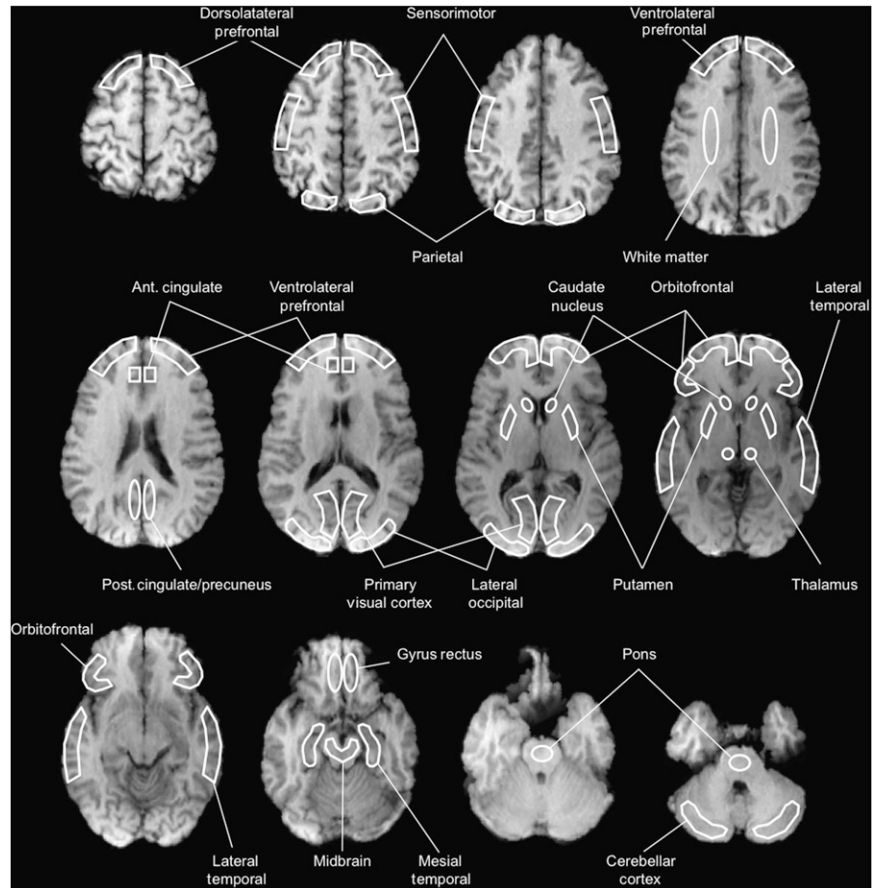


FIGURE 1. Schematic representation of ROI template defined on MR image. In white, with their respective labels, are enhanced examples of cortical and subcortical ROIs examined in this study. Also shown is the cerebellar cortex ROI used as reference region. Ant. = anterior; post. = posterior.

on the presence (green to red) or absence (blue to black) of ^{18}F -florbetaben binding in the cerebral cortex. After grouping together possible and probable from the visual assessment, a 2×2 contingency analysis was used to determine the test sensitivity and specificity of both semiquantitative and visual analysis of ^{18}F -florbetaben in differentiating probable AD patients from controls.

Statistical Evaluation

Normality of distribution was tested using the Shapiro–Wilk test and visual inspection of variable histograms. Statistical evaluations between groups were performed using a Tukey–Kramer honestly significant difference test to establish differences between group means and using a Dunnett test to compare each group with controls. Effect size was measured with Cohen *d*. Categorical differences were evaluated using Fisher exact test. Pearson product–moment correlation analyses were conducted between ^{18}F -florbetaben SUVR and clinical features. Given the association between $\text{A}\beta$ deposition and age observed with ^{11}C -PiB (27), all comparisons and correlations were corrected for age effects. Receiver-operating-characteristic (ROC) curve analysis was applied to assess the robustness of the different parameters to discriminate between AD patients and controls. Data are presented as mean \pm SD unless otherwise stated.

RESULTS

Participants’ demographics are detailed in Table 1. One hundred nine subjects were recruited and studied between September 2006 and June 2010. All recruited subjects com-

pleted the respective studies and are included in the evaluation. There were no significant differences between the different groups and controls in age or sex. Significantly lower MMSE scores were observed in the AD, DLB, and FTLD groups (Table 1). Of the 109 participants, 32 (29%) were classified as controls (MMSE, 29.6 ± 0.7), 30 (28%) fulfilled criteria for probable AD (MMSE, 22.8 ± 3.7), 20 (18%) fulfilled criteria for MCI (MMSE, 27.4 ± 1.9 , 80% amnesic type), 11 (10%) fulfilled criteria for FTLD (MMSE, 24.5 ± 2.9), 7 (6%) fulfilled criteria for DLB (MMSE, 24.0 ± 6.6), 5 (5%) fulfilled criteria for PD (MMSE, 27.4 ± 2.7), and 4 (4%) fulfilled criteria for VaD (MMSE, 27.8 ± 2.1). No serious adverse events related to the study drug were observed or reported by any participants as a result of the ^{18}F -florbetaben scans, even when low SAs were used. There were no significant fluctuations of hematology, biochemistry, coagulation profile, and vital signs in any subject from prescan laboratory blood samples and 1-wk postscan laboratory blood samples. No participant or any of their relatives raised concerns about the study, and all enrolled participants tolerated the study well.

All AD patients except for 1 showed extensive cortical ^{18}F -florbetaben retention that was greater in the frontal and posterior cingulate or precuneus cortex and slightly less in the lateral temporal and parietal cortex (Fig. 2). Similar to

TABLE 1
Demographics

Parameter	Controls (n = 32)	PD (n = 5)	DLB (n = 7)	MCI (n = 20)	AD (n = 30)	FTLD (n = 11)	VaD (n = 4)
Age (y)	70.7 ± 6.3	72.6 ± 6.5	71.7 ± 5.7	73.4 ± 6.7	72.0 ± 9.2	63.5 ± 7.0*	73.0 ± 11.0
Sex							
M	19	5*	7*	12	14	7	0*
F	13	0*	0*	8	16	4	4*
MMSE	29.6 ± 0.7	27.4 ± 2.7	24.0 ± 6.6*	27.4 ± 1.9	22.8 ± 3.7*	24.5 ± 2.9*	27.8 ± 2.1
Clinical dementia rating	0.0	0.3 ± 0.3*	0.8 ± 0.3*	0.5 ± 0.2*	1.0 ± 0.0*	1.0 ± 0.4*	0.6 ± 0.3*
Injected activity (MBq)	282 ± 47	294 ± 17	271 ± 31	295 ± 14	268 ± 41	301 ± 29	263 ± 39
Injected mass (μg)	1.2 ± 0.7	2.1 ± 1.0	2.2 ± 1.5	1.7 ± 0.7	1.5 ± 1.6	1.7 ± 1.5	2.4 ± 1.1

*Significantly different from controls ($P < 0.05$).

what was observed in ^{11}C -PiB studies, there was relative sparing of primary sensorimotor cortex, with no appreciable binding in the cerebellar cortex. High retention in white matter was observed in all groups.

Twenty-seven controls presented no cortical or subcortical gray-matter ^{18}F -florbetaben binding, and their scans were clearly distinguishable from patients with AD (Fig. 1). However, 5 (16%) controls were classified as having mild to diffuse cortical ^{18}F -florbetaben binding involving the orbitofrontal and cingulate or precuneus regions, in a pattern similar to that observed in AD and that resembled the early stages of A β deposition described by Braak and Braak (28).

Cortical ^{18}F -florbetaben binding was present in 12 (60%) of 20 MCI subjects (Fig. 2), with some of their PET scans visually indistinguishable from AD patients. Conversely, 8 MCI subjects showed only white-matter retention and were visually indistinguishable from controls. All 5 PD, 3 of 4 VaD, 10 of 11 FTLD, and 5 of 7 DLB patients had low cortical ^{18}F -florbetaben binding (Fig. 2). One FTLD patient showed mild frontal binding of ^{18}F -florbetaben, whereas 2 DLB patients presented with cortical binding with a distribution similar to that of AD. However, when present, the degree of ^{18}F -florbetaben binding in the DLB patients was generally lower than that observed in AD (Fig. 3). One VaD patient presented with a PET scan indistinguishable from AD.

As previously reported, distribution volume ratio (DVR) values derived from dynamic data correlated strongly with

SUVR in all cortical regions, with $r = 0.98$ and $P < 0.0001$ for the mean neocortical measure (14). Therefore, SUVR calculated from the data acquired over the 90- to 110-min postinjection interval are reported here.

Neocortical SUVR in controls was 1.26 ± 0.2 , compared with 1.93 ± 0.3 in AD patients ($P < 0.0001$, effect size $d = 2.8$). The box plot in Figure 3 shows the neocortical SUVR for all groups examined. Applying the cutoff SUVR of 1.4, 5 (16%) controls were considered to have high A β burden. The 5 PD patients had low neocortical SUVR, with no overlap with the AD patients. There was also good separation between the AD and FTLD groups, despite 1 high ^{18}F -florbetaben-binding FTLD and 1 low ^{18}F -florbetaben-binding AD patient (Fig. 3). Although 63% of the amnesic MCI subjects presented with high ^{18}F -florbetaben binding, the nonamnesic MCI subjects showed low ^{18}F -florbetaben binding.

All gray-matter regions in the AD group were significantly higher than in controls. Table 2 lists the regional SUVR for all groups. In the MCI group, the posterior cingulate, parietal, temporal, and frontal cortices and the striatum were significantly higher than in controls. No regional differences were observed between controls and the other groups examined.

ROC analysis of the visual reading of the AD and control ^{18}F -florbetaben PET images obtained 90–110 min after injection against clinical diagnosis yielded an area under the curve (AUC) of 0.92, with a sensitivity of 97% and a specificity of 88%. Semiquantitative analysis yielded an AUC of 0.91, with a sensitivity of 97% and a specificity

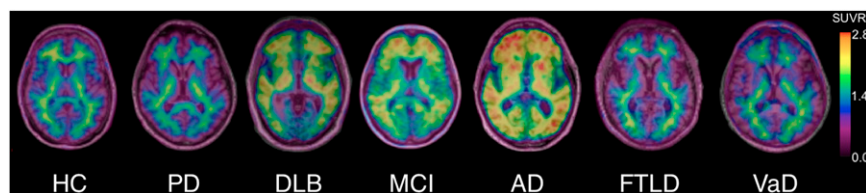
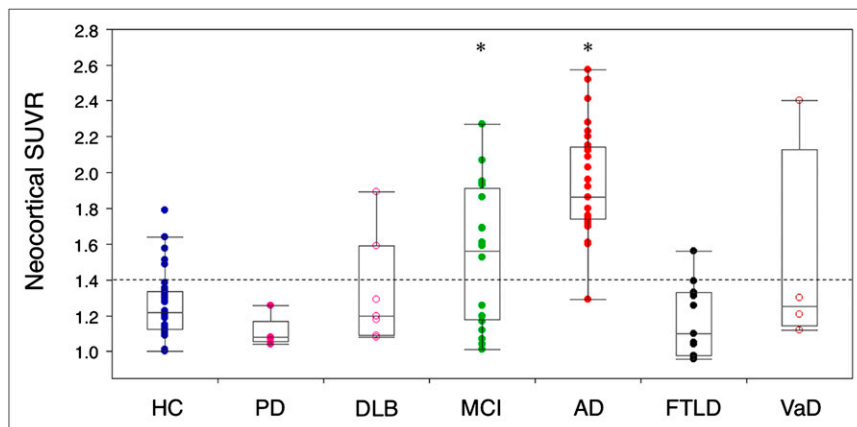


FIGURE 2. ^{18}F -florbetaben imaging with PET. Representative ^{18}F -florbetaben PET transaxial images overlaid on individual coregistered MR images of 68-y-old control (MMSE, 29), 73-y-old patient with PD (MMSE, 29), 73-y-old patient with DLB (MMSE, 10), 70-y-old subject with MCI (MMSE, 26), 80-y-old AD patient (MMSE,

25), 62-y-old patient with FTLD (MMSE, 25), and 79-y-old patient with VaD (MMSE, 26). PET images show clear differences when comparing cortical ^{18}F -florbetaben binding in controls, PD, VaD, and FTLD with MCI, DLB, or AD patients. Only nonspecific ^{18}F -florbetaben binding in white matter is observed in controls, PD, VaD, and FTLD, compared with ^{18}F -florbetaben binding in cortical areas of AD, MCI, and DLB patients. All images are scaled to same SUVR maximum. HC = controls.

FIGURE 3. In vivo quantification of neocortical A β burden with ^{18}F -florbetaben. Box and whiskers plots of A β burden by clinical classification. A β burden in AD and MCI groups was significantly higher (*) than in controls. About 60% of MCI subjects showed high florbetaben retention. Two of 7 DLB, 1 of 11 FTLD, and 1 of 4 VaD patients presented with high florbetaben retention although lower than that observed in AD. PD patients showed no cortical florbetaben retention. Dotted line = threshold (SUVR 1.4) between high and low florbetaben binding. HC = controls. *Significantly different from controls ($P < 0.05$).



of 84%. ROC analysis of the visual reading and semiquantitative analysis from the AD and FTLD patients yielded an AUC of 0.92, with a sensitivity of 97% and a specificity of 91%. When the same analysis was performed with the MCI subjects, AUCs of 0.74 and 0.80 were obtained against controls or AD participants, respectively.

There was no effect on scan appearance or neocortical SUVR from lowering the SA of ^{18}F -florbetaben (1.9 ± 0.2 GBq/ μmol to 58.4 ± 27.5 GBq/ μmol) in the subgroup of 8 AD patients and 8 controls who underwent repeated scans. Neocortical SUVR measured 1.32 ± 0.22 and 1.32 ± 0.25 ($P = 0.71$) for the 8 controls in the high- and low-SA scans, respectively, whereas in the 8 AD patients the neocortical SUVR measured 1.89 ± 0.36 and 1.91 ± 0.31 ($P = 0.65$) in the high- and low-SA scans, respectively. Test-retest variability for neocortical SUVR was 6.2% (range, 0.6%–12.2%; median, 6.6%) in AD patients and 2.9% (range,

0.1%–9.0%; median, 2.8%) in controls, with a combined variability of 4.6% for the whole subgroup.

Although there were no correlations between age and neocortical SUVR in the groups examined, a trend was observed in the control group ($r = 0.32$, $P = 0.09$). No differences were observed in neocortical SUVR between men and women when all groups were considered together. When examined separately, and although there were no differences in age and MMSE, male AD patients had significantly higher neocortical SUVR than their female counterparts (2.12 ± 0.26 vs. 1.78 ± 0.23 , $P = 0.001$). Neocortical SUVR correlated inversely with MMSE when all groups were analyzed together ($r = -0.49$, $P < 0.0001$) and only in the MCI group when examined separately ($r = -0.76$, $P < 0.0001$). There was no correlation in the AD or FTLD groups between neocortical SUVR and time elapsed between onset of cognitive impairment and development of

TABLE 2
Regional ^{18}F -Florbetaben Binding

Region	Controls (n = 32)	PD (n = 5)	DLB (n = 7)	MCI (n = 20)	AD (n = 30)	FTLD (n = 11)	VaD (n = 4)
Dorsolateral prefrontal	1.19 \pm 0.2	1.09 \pm 0.1	1.24 \pm 0.3	1.36 \pm 0.4	1.82 \pm 0.3*	1.10 \pm 0.2	1.43 \pm 0.6
Ventrolateral prefrontal	1.26 \pm 0.2	1.08 \pm 0.1	1.37 \pm 0.4	1.54 \pm 0.5*	2.02 \pm 0.3*	1.18 \pm 0.3	1.54 \pm 0.6
Orbitofrontal	1.31 \pm 0.2	1.11 \pm 0.1	1.38 \pm 0.3	1.56 \pm 0.4*	2.00 \pm 0.4*	1.21 \pm 0.2	1.59 \pm 0.8
Posterior cingulate	1.24 \pm 0.2	1.03 \pm 0.0	1.37 \pm 0.5	1.60 \pm 0.5*	2.05 \pm 0.4*	1.21 \pm 0.3	1.52 \pm 0.7
Anterior cingulate	1.20 \pm 0.2	0.90 \pm 0.1	1.19 \pm 0.3	1.45 \pm 0.5	1.95 \pm 0.4*	1.20 \pm 0.3	1.43 \pm 1.0
Parietal cortex	1.18 \pm 0.2	1.12 \pm 0.1	1.34 \pm 0.4	1.42 \pm 0.4*	1.82 \pm 0.3*	1.07 \pm 0.2	1.35 \pm 0.3
Occipital cortex	1.41 \pm 0.2	1.41 \pm 0.2	1.45 \pm 0.2	1.61 \pm 0.3	1.83 \pm 0.2*	1.27 \pm 0.1	1.59 \pm 0.3
Lateral temporal cortex	1.29 \pm 0.2	1.15 \pm 0.1	1.32 \pm 0.2	1.56 \pm 0.4*	1.96 \pm 0.3*	1.19 \pm 0.2	1.61 \pm 0.6
Mesial temporal cortex	1.23 \pm 0.1	1.14 \pm 0.1	1.21 \pm 0.2	1.26 \pm 0.2	1.40 \pm 0.2*	1.17 \pm 0.1	1.29 \pm 0.2
Caudate nuclei	1.32 \pm 0.2	1.24 \pm 0.1	1.49 \pm 0.4	1.63 \pm 0.5*	2.00 \pm 0.4*	1.24 \pm 0.2	1.48 \pm 0.6
Putamen	1.30 \pm 0.1	1.24 \pm 0.1	1.45 \pm 0.4	1.50 \pm 0.3*	1.81 \pm 0.3*	1.27 \pm 0.2	1.40 \pm 0.4
Thalamus	1.30 \pm 0.2	1.21 \pm 0.2	1.31 \pm 0.2	1.34 \pm 0.2	1.51 \pm 0.3*	1.27 \pm 0.2	1.30 \pm 0.2
Mid brain	1.75 \pm 0.2	1.88 \pm 0.3	1.89 \pm 0.2	1.74 \pm 0.1	1.81 \pm 0.3	1.65 \pm 0.3	1.97 \pm 0.3
Pons	1.97 \pm 0.2	2.06 \pm 0.3	1.93 \pm 0.1	1.96 \pm 0.2	1.93 \pm 0.4	1.80 \pm 0.2	2.10 \pm 0.4
White matter	1.97 \pm 0.2	1.82 \pm 0.2	1.86 \pm 0.1	1.95 \pm 0.2	1.93 \pm 0.4	1.80 \pm 0.3	1.95 \pm 0.2
Neocortex	1.26 \pm 0.2	1.14 \pm 0.1	1.38 \pm 0.3	1.52 \pm 0.4*	1.93 \pm 0.3*	1.18 \pm 0.1	1.51 \pm 0.6
Effect size (d)		0.9	0.8	0.8	2.8	0.4	0.6

*Significantly different from controls ($P < 0.05$).

the diagnostic clinical features, but a trend was observed in the DLB group ($r = -0.66$, $P = 0.15$).

DISCUSSION

This is the first report, to our knowledge, in which 109 participants encompassing a wide range of dementing and nondementing neurodegenerative diseases were evaluated with an ^{18}F -labeled A β imaging radiotracer. The studies were designed to assess the specificity of ^{18}F -florbetaben to detect AD pathology in clinically well-characterized cases.

The AD group showed higher A β burden, as defined by ^{18}F -florbetaben binding, than did controls, in accordance with previous reports using ^{18}F -florbetaben or other amyloid tracers (2,3,14–16). Only 1 of the 30 participants classified as AD had low ^{18}F -florbetaben binding. A potential limitation of our study is the reliance on clinical diagnosis as the gold standard rather than neuropathology. Thus, our finding may be attributable to incorrect clinical diagnosis because, even in highly specialized centers, the accuracy of clinical diagnosis, compared with postmortem histopathologic diagnosis, is around 85%–90% (29–31).

In contrast with our previous reports using ^{11}C -PiB (27), the relationship between age and neocortical SUVR in controls did not reach significance, most likely attributable to the low number of controls with elevated ^{18}F -florbetaben binding. On the other hand, and in agreement with that same report (27), the A β burden in AD patients was significantly higher in men than in women, suggesting that for similar cognitive impairment, women may be more susceptible to the effects of A β , requiring a lower A β burden to manifest dementia.

Only 16% of controls were deemed positive for A β in these studies. As in numerous reports, this finding suggests that A β deposition is an early feature of the disease preceding cognitive impairment. On the other hand, the prevalence of positive scans is slightly lower than the 20%–30% of positive scans in healthy elderly individuals reported using ^{11}C -PiB (2,4,32,33) and with postmortem studies that have documented moderate numbers of A β plaques in the cerebral cortex of about a quarter of nondemented persons aged over 75 y (34,35). Our findings are in accordance with previous reports using ^{11}C -PiB in MCI (60% positive) and FTLD (9% positive) (2,5). As with ^{11}C -PiB, ^{18}F -florbetaben PET appears to be an excellent test for distinguishing FTLD from AD. Ongoing longitudinal studies will determine whether the 2 well-differentiated clusters of ^{18}F -florbetaben binding in the MCI group can reliably predict those who will progress to AD or other causes of dementia. All PD patients and 5 of the 7 DLB patients showed low ^{18}F -florbetaben binding. The findings in the DLB group are somewhat at odds with previous reports using ^{11}C -PiB, in which more than 50% of the DLB patients showed A β deposition (36,37), though postmortem reports have shown wide variation where between 30% and 90% of DLB patients have shown A β plaques at autopsy (38). Con-

versely, and as we previously reported (2), there seems to be a strong association between rapid development of the full DLB phenotype and A β burden, with evidence that A β exacerbates α -synuclein-dependent neuronal injury (39). Therefore, strategies aimed at reducing A β in AD may also be beneficial in DLB patients.

Although the cortical distribution of ^{18}F -florbetaben is almost identical to that reported for ^{11}C -PiB, the degree of binding is slightly less. ^{18}F -florbetaben neocortical SUVR for AD was 53% greater than in controls. Our previously reported experience with ^{11}C -PiB, using the same equipment and semiquantitative methods, is that on average ^{11}C -PiB binding is 60%–70% higher in AD patients than in controls (2,27). Despite this, ^{18}F -florbetaben yielded a slightly larger effect size (2.8 vs. 2.2) probably because of the lower prevalence of high A β burden in the control group (33% vs. 16% for ^{11}C -PiB and ^{18}F -florbetaben, respectively). When compared with the available data from the other ^{18}F compounds (15,16), the effect size for ^{18}F -flutemetamol (2.7) and ^{18}F -florbetapir (2.3) is slightly lower than for ^{18}F -florbetaben.

Another important factor that might explain the slight discrepancy in specificity favoring the visual assessment over the semiquantitative approach is the degree of nonspecific binding to white matter. All ^{18}F compounds show higher nonspecific binding to white matter than ^{11}C -PiB. Although the ratios of frontal cortex to white matter for PiB are 0.8, 1.1, and 1.3 in controls, MCI, and AD, respectively (27), the same ratios for ^{18}F -florbetaben (0.7, 0.8, and 1.1), ^{18}F -flutemetamol (0.4, 0.5, and 0.7) (16), and ^{18}F -florbetapir (0.7 and 1.1 for controls and AD, respectively) (15) are lower.

The distribution of ^{18}F -florbetaben binding matched the postmortem distribution of neuritic plaques in AD (28), providing a robust separation of AD patients from controls and from patients with FTLD or PD. This separation was achieved either with visual image inspection or a simple semiquantitative measure derived from a short scan at 90 min after injection of the tracer. These findings suggest that ^{18}F -florbetaben PET can be used in clinical practice, with a short scan easily tolerated by elderly patients while allowing economical use of a PET camera. Furthermore, the decay half-life of ^{18}F makes centralized production with distribution to multiple PET sites possible, thereby improving access to A β imaging, enabling early and more accurate diagnosis of AD and the ability to conduct and monitor large-scale, multicenter, therapeutic clinical trials and simultaneously reducing the cost. Moreover, the reproducibility of the ^{18}F -florbetaben scans was estimated to be approximately 5%, even when 25 times greater amounts of cold florbetaben were injected, suggesting that within a wide range of SAs ^{18}F -florbetaben is a reliable tool for the in vivo assessment of A β deposition.

As observed with ^{11}C -PiB (2), only when all groups were considered together was there a correlation between neocortical SUVR and MMSE—a correlation driven by the low

A β burden in controls at one end and the high A β burden in AD at the other. We did not find a correlation between the A β burden and MMSE in the AD cases, in agreement with our previous reports with ¹¹C-PiB (2), and with postmortem studies that have not consistently demonstrated a relationship between the density of A β plaques and the severity of dementia (35,40,41). Our data suggest that A β deposition is an early event and likely to occur before demonstrable cognitive impairment. Similar to what has been reported using ¹¹C-PiB (9), a correlation between ¹⁸F-florbetaben binding and cognitive impairment was observed in MCI subjects. This finding has not been consistent (25), especially when only amnesic MCI subjects are examined. In the present sample, 20% of the MCI participants were classified as nonamnesic, and they presented with no A β burden, therefore driving the correlation between MMSE and ¹⁸F-florbetaben binding within the MCI group. Another important aspect is that 37% of amnesic MCI subjects did not have elevated ¹⁸F-florbetaben binding, suggesting that subject selection for anti-amyloid therapeutic trials in MCI by current clinical criteria will include a large proportion of subjects that are unlikely to have AD pathology.

Longitudinal A β imaging studies have shown that A β deposition is associated with a higher risk of cognitive decline in controls and MCI, denoting the nonbenign nature of A β deposition (10,42). Therefore the specificity of A β imaging with ¹⁸F-florbetaben for detection of AD is likely to increase with longer follow-up of study participants. Longitudinal follow-up will also determine the value of ¹⁸F-florbetaben PET for detection of prodromal and even preclinical AD (10,27). A β imaging is a tool that will open up new possibilities for early intervention and prevention of dementia due to AD. A β imaging is likely to play a critical role in the development of anti-amyloid therapies by improving patient selection at early phases of the disease and monitoring treatment response.

CONCLUSION

Our results demonstrate that ¹⁸F-florbetaben can reliably detect A β deposition in the brain and is thereby useful in the early and differential diagnosis of AD from other dementing or nondementing neurodegenerative conditions. ¹⁸F-florbetaben provides images similar to those provided by ¹¹C-PiB, without the limitation of the short ¹¹C radioactive decay half-life that precludes the application of PiB in clinical practice. Longitudinal studies with ¹⁸F-florbetaben will provide information on the rate of A β deposition, further clarifying the relationship between A β accumulation and cognitive decline and asserting the value of A β imaging as a predictor of cognitive decline and progression to clinical Alzheimer disease.

DISCLOSURE STATEMENT

The costs of publication of this article were defrayed in part by the payment of page charges. Therefore, and solely

to indicate this fact, this article is hereby marked "advertisement" in accordance with 18 USC section 1734.

ACKNOWLEDGMENTS

We thank Michael Woodward, Dr. John Merory, Dr. Peter Drysdale, Kenneth Young, Dr. Sylvia Gong, Fiona Lamb, Tanya Petts, Jessica Sagona, and Jason Bradley and the Brain Research Institute for their assistance with this study. This work was supported in part by grant 509166 of the National Health and Medical Research Council of Australia, Bayer Schering Pharma AG, the Austin Hospital Medical Research Foundation, and Neurosciences Victoria. No other potential conflict of interest relevant to this article was reported.

REFERENCES

1. Villemagne VL, Fodero-Tavoletti MT, Pike KE, Cappai R, Masters CL, Rowe CC. The ART of loss: abeta imaging in the evaluation of Alzheimer's disease and other dementias. *Mol Neurobiol*. 2008;38:1–15.
2. Rowe CC, Ng S, Ackermann U, et al. Imaging beta-amyloid burden in aging and dementia. *Neurology*. 2007;68:1718–1725.
3. Klunk WE, Engler H, Nordberg A, et al. Imaging brain amyloid in Alzheimer's disease with Pittsburgh Compound-B. *Ann Neurol*. 2004;55:306–319.
4. Mintun MA, Larossa GN, Sheline YI, et al. [¹¹C]PIB in a nondemented population: potential antecedent marker of Alzheimer disease. *Neurology*. 2006;67:446–452.
5. Rabinovici GD, Furst AJ, O'Neil JP, et al. ¹¹C-PIB PET imaging in Alzheimer disease and frontotemporal lobar degeneration. *Neurology*. 2007;68:1205–1212.
6. Ng SY, Villemagne VL, Masters CL, Rowe CC. Evaluating atypical dementia syndromes using positron emission tomography with carbon 11 labeled Pittsburgh Compound B. *Arch Neurol*. 2007;64:1140–1144.
7. Fagan AM, Mintun MA, Mach RH, et al. Inverse relation between in vivo amyloid imaging load and cerebrospinal fluid Abeta₄₂ in humans. *Ann Neurol*. 2006;59:512–519.
8. Chetelat G, Villemagne VL, Bourgeat P, et al. Relationship between atrophy and beta-amyloid deposition in Alzheimer disease. *Ann Neurol*. 2010;67:317–324.
9. Pike KE, Savage G, Villemagne VL, et al. Beta-amyloid imaging and memory in non-demented individuals: evidence for preclinical Alzheimer's disease. *Brain*. 2007;130:2837–2844.
10. Villemagne VL, Pike KE, Chetelat G, et al. Longitudinal assessment of Abeta and cognition in aging and Alzheimer disease. *Ann Neurol*. 2011;69:181–192.
11. Dubois B, Feldman HH, Jacova C, et al. Research criteria for the diagnosis of Alzheimer's disease: revising the NINCDS-ADRDA criteria. *Lancet Neurol*. 2007;6:734–746.
12. Dubois B, Feldman HH, Jacova C, et al. Revising the definition of Alzheimer's disease: a new lexicon. *Lancet Neurol*. 2010;9:1118–1127.
13. Villemagne VL, Rowe CC. Amyloid PET ligands for dementia. *PET Clin*. 2010;5:33–53.
14. Rowe CC, Ackerman U, Browne W, et al. Imaging of amyloid beta in Alzheimer's disease with ¹⁸F-BAY94-9172, a novel PET tracer: proof of mechanism. *Lancet Neurol*. 2008;7:129–135.
15. Wong DF, Rosenberg PB, Zhou Y, et al. In vivo imaging of amyloid deposition in Alzheimer disease using the radioligand ¹⁸F-AV-45 (florbetapir F 18). *J Nucl Med*. 2010;51:913–920.
16. Vandenberghe R, Van Laere K, Ivanoiu A, et al. ¹⁸F-flutemetamol amyloid imaging in Alzheimer disease and mild cognitive impairment: a phase 2 trial. *Ann Neurol*. 2010;68:319–329.
17. Jureus A, Swahn BM, Sandell J, et al. Characterization of AZD4694, a novel fluorinated Abeta plaque neuroimaging PET radioligand. *J Neurochem*. 2010;114:784–794.
18. Petersen RC, Smith GE, Waring SC, Ivnik RJ, Tangalos EG, Kokmen E. Mild cognitive impairment: clinical characterization and outcome. *Arch Neurol*. 1999;56:303–308.
19. McKhann G, Drachman D, Folstein M, Katzman R, Price D, Stadlan EM. Clinical Diagnosis of Alzheimer's Disease: report of the NINCDS-ADRDA Work Group under the auspices of Department of Health and Human Services Task Force on Alzheimer's Disease. *Neurology*. 1984;34:939–944.

20. Cairns NJ, Bigio EH, Mackenzie IR, et al. Neuropathologic diagnostic and nosologic criteria for frontotemporal lobar degeneration: consensus of the Consortium for Frontotemporal Lobar Degeneration. *Acta Neuropathol.* 2007;114:5–22.
21. McKeith IG, Galasko D, Kosaka K, et al. Consensus guidelines for the clinical and pathologic diagnosis of dementia with Lewy bodies (DLB): report of the consortium on DLB international workshop. *Neurology.* 1996;47:1113–1124.
22. Gelb DJ, Oliver E, Gilman S. Diagnostic criteria for Parkinson disease. *Arch Neurol.* 1999;56:33–39.
23. Roman GC, Tatemichi TK, Erkinjuntti T, et al. Vascular dementia: diagnostic criteria for research studies: report of the NINDS-AIREN International Workshop. *Neurology.* 1993;43:250–260.
24. Good CD, Johnsrude IS, Ashburner J, Henson RN, Friston KJ, Frackowiak RS. A voxel-based morphometric study of ageing in 465 normal adult human brains. *Neuroimage.* 2001;14:21–36.
25. Jack CR Jr., Lowe VJ, Senjem ML, et al. ¹¹C PiB and structural MRI provide complementary information in imaging of Alzheimer's disease and amnesic mild cognitive impairment. *Brain.* 2008;131:665–680.
26. Ng S, Villemagne VL, Berlangieri S, et al. Visual assessment versus quantitative assessment of ¹¹C-PIB PET and ¹⁸F-FDG PET for detection of Alzheimer's disease. *J Nucl Med.* 2007;48:547–552.
27. Rowe CC, Ellis KA, Rimajova M, et al. Amyloid imaging results from the Australian Imaging, Biomarkers and Lifestyle (AIBL) study of aging. *Neurobiol Aging.* 2010;31:1275–1283.
28. Braak H, Braak E. Frequency of stages of Alzheimer-related lesions in different age categories. *Neurobiol Aging.* 1997;18:351–357.
29. Gearing M, Mirra SS, Hedreen JC, Sumi SM, Hansen LA, Heyman A. The Consortium to Establish a Registry for Alzheimer's Disease (CERAD). Part X. Neuropathology confirmation of the clinical diagnosis of Alzheimer's disease. *Neurology.* 1995;45:461–466.
30. Lim A, Tsuang D, Kukull W, et al. Clinico-neuropathological correlation of Alzheimer's disease in a community-based case series. *J Am Geriatr Soc.* 1999;47:564–569.
31. Rasmussen DX, Brandt J, Steele C, Hedreen JC, Troncoso JC, Folstein MF. Accuracy of clinical diagnosis of Alzheimer disease and clinical features of patients with non-Alzheimer disease neuropathology. *Alzheimer Dis Assoc Disord.* 1996;10:180–188.
32. Aizenstein HJ, Nebes RD, Saxton JA, et al. Frequent amyloid deposition without significant cognitive impairment among the elderly. *Arch Neurol.* 2008;65:1509–1517.
33. Villemagne VL, Pike KE, Darby D, et al. Abeta deposits in older non-demented individuals with cognitive decline are indicative of preclinical Alzheimer's disease. *Neuropsychologia.* 2008;46:1688–1697.
34. Bennett DA, Schneider JA, Arvanitakis Z, et al. Neuropathology of older persons without cognitive impairment from two community-based studies. *Neurology.* 2006;66:1837–1844.
35. Price JL, Morris JC. Tangles and plaques in nondemented aging and "preclinical" Alzheimer's disease. *Ann Neurol.* 1999;45:358–368.
36. Gomperts SN, Rentz DM, Moran E, et al. Imaging amyloid deposition in Lewy body diseases. *Neurology.* 2008;71:903–910.
37. Edison P, Rowe CC, Rinne JO, et al. Amyloid load in Parkinson's disease dementia and Lewy body dementia measured with [¹¹C]PIB positron emission tomography. *J Neurol Neurosurg Psychiatry.* 2008;79:1331–1338.
38. Hansen LA, Samuel W. Criteria for Alzheimer's disease and the nosology of dementia with Lewy bodies. *Neurology.* 1997;48:126–132.
39. Masliah E, Rockenstein E, Veinbergs I, et al. Beta-amyloid peptides enhance alpha-synuclein accumulation and neuronal deficits in a transgenic mouse model linking Alzheimer's disease and Parkinson's disease. *Proc Natl Acad Sci USA.* 2001;98:12245–12250.
40. Naslund J, Haroutunian V, Mohs R, et al. Correlation between elevated levels of amyloid beta-peptide in the brain and cognitive decline. *JAMA.* 2000;283:1571–1577.
41. Prohovnik I, Perl DP, Davis KL, Libow L, Lesser G, Haroutunian V. Dissociation of neuropathology from severity of dementia in late-onset Alzheimer disease. *Neurology.* 2006;66:49–55.
42. Morris JC, Roe CM, Grant EA, et al. Pittsburgh Compound B imaging and prediction of progression from cognitive normality to symptomatic Alzheimer disease. *Arch Neurol.* 2009;66:1469–1475.